J Therm Anal Calorim (2012) 107:717–723
DOI 10.1007/s10973-011-1776-2

The influence of wood flour and compatibilizer (*m*-TMI-*g*-PP) on crystallization and melting behavior of polypropylene

Liping Li · Qingwen Wang · Chuigen Guo

Received: 25 January 2011 / Accepted: 27 June 2011 / Published online: 17 July 2011

Abstract Wood flour/polypropylene composites (WPC) were prepared by melt extruding with different wood flour (WF) loadings. The non-isothermal crystallization and melting was studied with different WF loadings, for W40P60 and W40P60M6, the melting was investigated after non-isothermal and isothermal crystalline. Comparing with neat polypropylene, the melting behavior of the composites, both non-isothermally and isothermally, was investigated by differential scanning calorimetry (DSC). The results showed that WF was an effective heterogeneous nucleating agent, as evidenced by an increase in the crystallization temperature and the crystallinity for melt crystallization of PP with increasing WF content. For the non-isothermal samples, the origins of the double melting behaviors were discussed, based on the DSC results of PP. The XRD measurements confirmed that no crystalline transition existed during the non-isothermal crystallization process. With *m*-TMI-*g*-PP adding, due to compatibilization phenomenon were probably responsible for decreasing T_m, X_c. In the DSC scan after isothermal crystallization process, the single melting behaviors were found and each melting endotherm had a different origin.

Keywords Poly(propylene) (PP) · Compatibilization · Crystallization · Melt

L. Li
Heilongjiang Key Laboratory of Molecular Design and Preparation of Flame Retarded Materials, College of Science, Northeast Forestry University, Harbin 150040, China

Q. Wang · C. Guo (✉)
MOE Key Laboratory of Bio-based Material Science and Technology, Ministry of Education, Northeast Forestry University, Harbin 150040, China
e-mail: guochuigen@nefu.edu.cn

Introduction

Wood–plastic composites (WPC) have been rapidly developed and widely applied in packaging, household articles, furniture, office appliances, building, and automotive industry [1–4]. It is well known that the mechanical and physical properties of WPC products are affected by a number of factors, such as particle size of wood, the strength of the wood particles, the volume fraction, and aspect ratio of fiber, fiber orientation, dispersion level, fiber–polymer adhesion, mixing time, and processing temperature [5–8]. Among these factors, fiber–fiber interactions as well as the fiber–matrix adhesion plays the most important role in transferring the stress from the matrix to the filler, wood flour (WF) has a relatively low surface tension, low surface tension results in low interfacial tension and reversible work of adhesion, thus particle–particle and particle–matrix interactions decrease as well, and this greatly reduces the potential of natural fibers to be used as reinforcement for polymers [9–11].

Different techniques have been employed to resolve this problem [12–15], such as, chemical modification of the fiber or the addition of compatibilizing agents to enhance the interfacial adhesion, and increase the mechanical and physical properties of polypropylene (PP)/wood–fiber composites. The study showed that adding maleated PP (MA-PP) can significantly improves the bio-fiber or flour/matrix bonding [16–19]. Qiu et al. [20] reported that the interfacial adhesion can be improved by adding isocyanate (1,6-diisocyanatohexane) as a compatibilizing agent in PP/cellulose composite as well as MA-PP/cellulose composite. Karmarkar [21] and Guo [22] have reported improved mechanical properties by using isocyanate coupling agent (*m*-TMI-*g*-PP). In this study, a compatibilizer with isocyanate functional group *m*-TMI-*g*-PP was used to improve the adhesion between WF and PP.

In recent years, for the WPC composites, the emphasis of studies has been placed on water absorption, mechanical properties, thermal decomposition, weathering, crystallization, and rheological properties in the presence of compatibilizing agents [22–26]. There are many articles on studying the crystallization behavior of PP or PP composites [27–31]. The crystallization behavior of reinforced-PP composites with flax fiber, sisal fiber, pine fiber, glass fiber, hemp fiber, jute fiber, and wood have been also reported [25, 32–37]. In addition, crystallization behavior represents an interesting research subject to optimize process conditions and control the properties of the final products. Especially, non-isothermal crystallization of polymers, which is great technological significance, since most practical processing techniques proceed under non-isothermal conditions. These fundamental studies are essential to understand the solid-state properties of these materials. However, there are few reports about such investigations of the non-isothermal and isothermal crystallization and melting behavior of WF/PP composites, especially in the presence of *m*-TMI-*g*-PP. Therefore, fundamental studies on the effect of the presence of WF and with *m*-TMI-*g*-PP as a compatibilizer on the crystallization and melting behavior of PP are of great importance from both a theoretical and practical point of view. In this article, the isothermal and non-isothermal crystallization behaviors of WF/PP were carried out by differential scanning calorimetry (DSC); the melting behaviors following isothermal and non-isothermal crystallization process were discussed. The crystal structure was characterized by X-ray diffraction (XRD).

Experimental

Materials

PP [density 0.89–0.91 g cm^{-3}, the melting flow index of 8 g $(10\ min)^{-1}$ at 503 K, 2.16 kg] used as the matrix of the composites was supplied by DaQing PetroChemical Company. WF with 40–60 mesh were supplied by Harbin Yongxu Co. Ltd. WF were dried at 378 K for 24 h to remove moisture and then stored over in sealed containers. *m*-isopropenyl-α,α-dimethylbenzyl isocyanate(*m*-TMI) was manufactured by Cytec corporation, dicumyl peroxide (DCP) was manufactured by Tianjin Guangfa company, *m*-TMI-*g*-PP used as compatibilizing agent for WF/PP composites was prepared by our laboratory.

Sample preparation

In order to study the crystalline behavior of WF loading on the properties of WPC, Table 1 gives the compositions of all the investigated systems. The mixture of WF, PP, and *m*-TMI-*g*-PP was mixed in a high speed mixer for 8 min, subsequently melted, and extruded by the twin-screw/single-screw two-step extruder system and formed sheets for testing. The processing temperature for extrusion was set at 423 K for melting zone, 443–453 K for pumping zone and 448 K for die zone, respectively. The rotary speed of twin-screw was 100 rpm.

Table 1 Composition of PP and its composites

No.	Designation	WF/%	PP/%	*m*-TMI-*g*-PP/%
0	Pure PP	0	100	0
1	W10P90M6	10	90	6
2	W20P80M6	20	80	6
3	W30P70M6	30	70	6
4	W40P60M6	40	60	6
5	W50P50M6	50	50	6
6	W40P60	40	60	0

Non-isothermal crystallization process

Non-isothermal crystallizations of all samples were carried out on a Perkin-Elmer Diamond DSC. The sample was rapidly heated at a rate of 100 K min^{-1} to 463 K, stayed there for 10 min to eliminate thermal and mechanical prehistory, for the samples no. 0–5, the samples were cooled to 298 K at cooling rates of 10 K min^{-1}. In order to investigate the effect of wood four and *m*-TMI-*g*-PP on non-isothermal and isothermal melting, PP, W40P60, and W40P60M6 were chosen for comparative study. The sample nos. 0, 4, 6 was cooled to 298 K at cooling rates of 5, 10, 15, 20, and 40 K min^{-1} and finally heated again to 463 K (i.e., 2nd heating) at a rate of 10 K min^{-1}. The exothermic curves of heat flow as a function of temperature were recorded to analyze the non-isothermal crystallization of PP and its composites. All the experiments were carried out under pure nitrogen.

Isothermal crystallization process

The samples (0, 4, 6) were rapidly heated at a rate of 100 K min^{-1} to 463 K, stayed there for 10 min to eliminate thermal and mechanical prehistory, and then rapidly cooled to the designated crystallization temperature (T_c) at a rate of 100 K min^{-1}, which were five different temperatures in the range of 387–401 K for each sample in the isothermal crystallization process, and held at this temperature for 15 min until crystallization was completed. The specimens were subsequently heated to 463 K at a rate of 10 K min^{-1}. All the experiments were carried out under pure nitrogen.

Table 2 The parameters determined from the DSC exothermal curves

Samples	PP[a] ΔH_m/J g^{-1}	X_c/%	T_m/K	T_o/K	T_p/K	T_e/K
PP	43.8	29.6	432.9/437.3	392.2	384.5	379.5
W10P90M6	50.7	34.3	435.3	397.7	390.7	386.0
W20P80M6	75.3	50.9	435.3	398.2	391.3	387.2
W30P70M6	90.8	61.3	435.3	399.8	393.3	389.1
W40P60M6	90.9	61.4	435.6	401.7	393.9	394.3
W50P50M6	91.2	61.6	436.6	401.8	394.3	390.3

[a] Values normalized to the amount of the PP phase

XRD analysis

XRD patterns were recorded by using a Bruker GADDS diffractometer, with an area detector operating under 40 kV and 40 mA, using Cu Kα radiation ($\lambda = 0.154$ nm).

The scanning rate was 4° min^{-1}. Sample plates with dimensions 1 × 1 × 0.05 cm^3 were prepared using two hot compression molding in a press at a temperature of 463 K and then cooled to the room temperature at the rate of 10 K min^{-1}. During the measurements the sample was protected by a flow of inert gas (helium) to prevent the oxidation at high temperature.

Results and discussion

Heating–cooling cycles

After being kept at 463 K for 10 min to remove any thermal and mechanical prehistory, all of the melt samples were cooled at 10 K min^{-1} to 298 K. Figure 1 shows the cooling and 2nd heating scans for neat PP and it's composite with different WF content at 10 K min^{-1} heating rate. The cooling peak temperature (T_p), the onset temperature of crystallization (T_o), the end temperature of crystallization (T_e), melting temperature(T_m), melt crystallization enthalpies (ΔH_m), degree of crystallinity (X_c) are listed in Table 2. The values of T_m and ΔH_m were obtained from the maxima and the area of the melting peaks, respectively. The values of ΔH_m were normalized to the amount of the PP phase. The X_c [38] is defined as the ratio of ΔH_m to ΔH_m^0, ΔH_m^0 of perfect PP crystals has been reported as 148 J g^{-1} [39].

The degree of supercooling reduced and the crystallization rate increased with increasing WF loading, T_o and T_p were shifted to higher temperature. The neat PP crystallized very slowly that was observed at 384.5 K. For the composites, higher crystallization peaks were observed at about 390–394.3 K, whose positions slightly increased as the WF content increased. In addition, the ΔH_m of the composites were much larger than that of the neat PP, and gradually increased with increasing WF content, also indicating a heterogeneous nucleation effect of WF for melt crystallization. This indicated that the WF induced the formation of crystals as heterogeneous nucleation sites, thus promoting the crystallization rate and degree of crystallinity in the composites. The same observation was reported in flax fiber/PP [12, 32]. From Fig. 1 and Table 2, it could be seen that the PP had double melting peaks and composites only one peak and these parameters were variable at different WF content.

At high-temperature regions, the PP showed a main melting peak and a shoulder at higher temperature, the peak of higher temperature was minor than that of lower temperature. The formation of two melting peaks attributed to the secondary crystallization of PP. And a single melting peak was observed at around 435.3–436.6 K for composites, with increasing WF content, the magnitude of T_m significantly decreased, together with a slight position shift toward higher temperatures, so indicating that recrystallization was significantly prohibited upon incorporation of WF with the matrix. The more contents the WF, the more influence on crystallization of PP. So, it was easy to

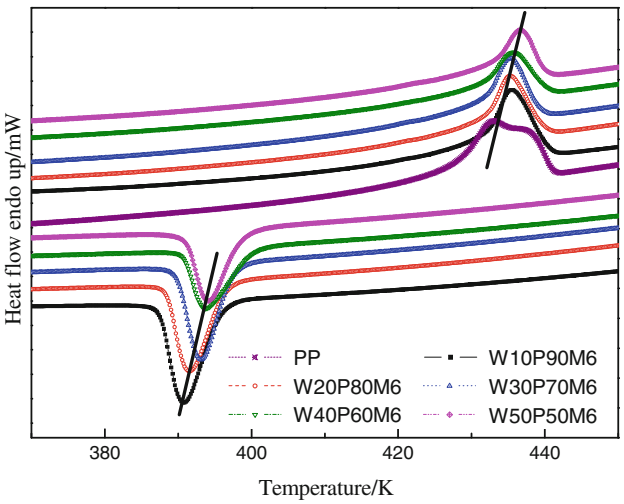

Fig. 1 DSC cooling–melting curves of different WF content at 10 K min^{-1}

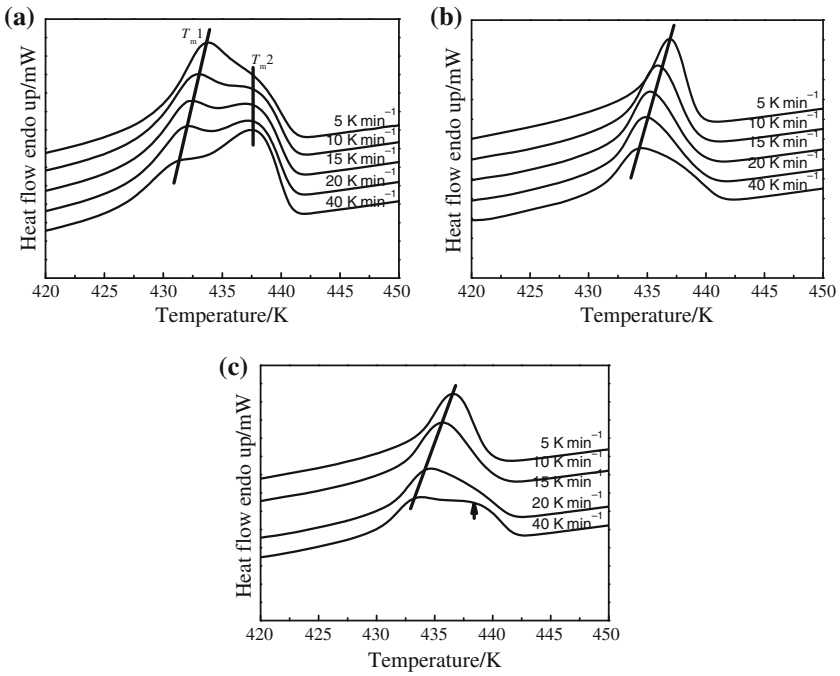

Fig. 2 The DSC thermograms of samples after non-isothermal crystallization at different cooling rates at a heating rate of 10 K min^{-1}: **a** PP; **b** W40P60; and **c** W40P60M6

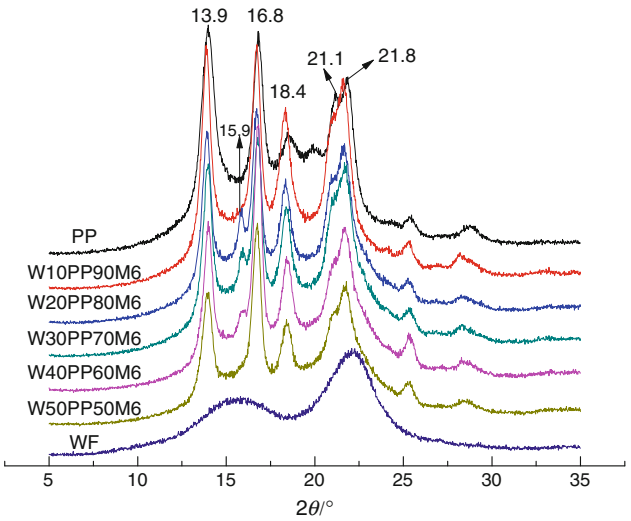

Fig. 3 X-ray diffractograms for PP and its composites

crystallize into perfect and stable crystals for PP, and the melting temperature shifted to higher temperature. This phenomenon supported the role of the nucleating sites, as played by the WF.

Melting behavior following nonisothermal crystallization

Figure 2 showed melting endotherms of PP and its composites after non-isothermally crystallization at five different cooling rates, ranging from 5 to 40 K min^{-1} and melting curves were recorded at a fixed heating rate of 10 K min^{-1}. Apparently, the double melting behavior was observed for the neat PP, the low melting peak temperature (T_m1) shifted toward a lower temperature with increasing cooling rate; the intensity of the peak T_m1 became weaker and weaker. While, the high melting temperature (T_m2) remained almost constant the intensity of the peak T_m2 became stronger and stronger. The occurrence of the low temperature melting endotherm should correspond to the melting of the crystallites originally formed during a cooling scan. The T_m1 values decreased with increasing cooling rate, which implied that the crystallites formed during a fast cooling scan were less stable than those formed during a slower cooling scan. Upon heating, the less stable crystals melt to a supercooled state in which recrystallization could take place very rapidly with the formation of better crystals. The final melting of recrystallized material took place at the same temperature, regardless of the non-isothermal crystallization rate at which the crystals were originally formed [40]. The occurrence of the high-temperature melting endotherm was postulated to be a result of the melting of the recrystallized materials formed during a heating scan [41]. This is because the polymer chains have not enough time to reorganize into ordered structures (crystals) at the higher heating rate, that is, recrystallization is somewhat repressed. Namely, recrystallization is a time and temperature-dependent process, thus decreasing the heating rate increases the proportion of a more perfectly formed structure with a higher melting temperature. Consequently, a reduced heating rate leads to greater expressed peak duplication and to a higher peak at the higher temperature [31]. Therefore, it could be concluded that the crystals

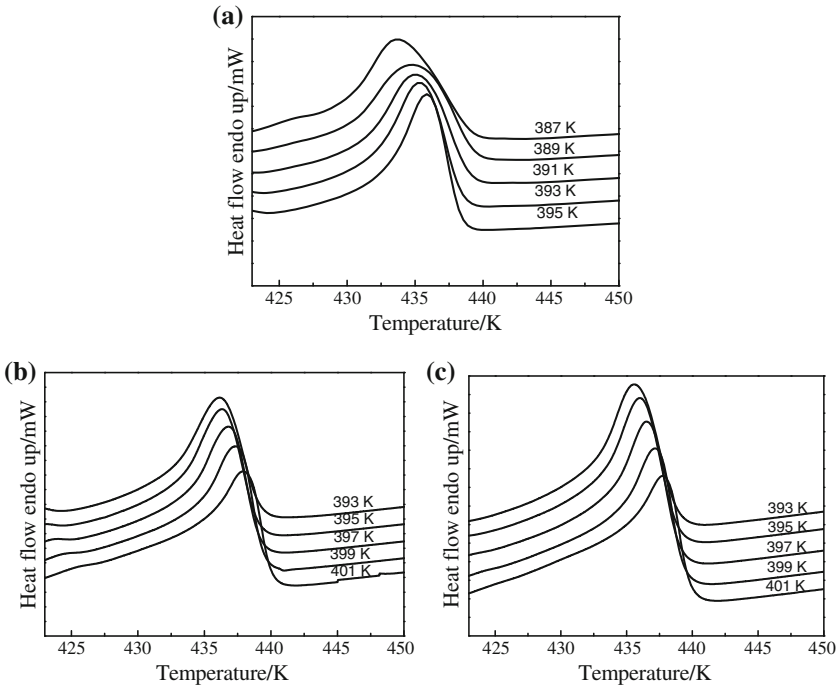

Fig. 4 The DSC thermograms of samples after isothermal crystallization at indicated temperature for 15 min at a heating rate of 10 K min^{-1}: **a** PP; **b** W40P60; and **c** W40P60M6

Table 3 Values of melting point and melting enthalpy of PP and its composites melting at a heating rate of 10 K min^{-1} after isothermal crystallization at indicated temperature

	T_c/K	387	389	391	393	395	397	399	401
PP	T_m/K	433.7	435.0	435.1	435.4	435.9	–	–	–
	ΔH_m/J g^{-1}	56.29	53.27	51.86	52.19	51.89	–	–	–
	X_c/%	38.03	35.99	35.04	35.26	35.06			
W40P60	T_m/K	–	–	–	436.1	436.3	436.8	437.4	437.9
	ΔH_m/J g^{-1}	–	–	–	61.80	62.86	63.56	65.91	65.65
	X_c/%				41.75	42.47	42.94	44.53	44.36
W40P60M6	T_m/K	–	–	–	435.6	436.0	436.5	437.2	437.8
	ΔH_m/J g^{-1}	–	–	–	48.78	47.96	48.20	46.88	45.92
	X_c/%				32.96	32.40	32.56	31.67	31.03

Values normalized to the amount of the PP phase

which contributed to T_m2 partially originated from the re-crystallized population formed during the heating process. It was worth mentioning that WF reduced the tendency to recrystallization, for WF/PP composites, only a single melting endotherm was seen, which showed WF accelerate the crystalline rate and form perfect crystal. In Fig. 2c, it was interesting that a shoulder peak appeared at higher temperature(438.6 K) for melting curve of at 40 K min^{-1} cooling rate, showing *m*-TMI-*g*-PP improved WF/PP interactions that restricted the mobility of PP chains and hindered the crystallization process and appeared secondary crystallization.

Since the thermal history was identical for all of the neat and composite samples, in view of the absence of T_m2 for composites it was suggested that the T_m2 observed in the PP probably originated from melting of the imperfect crystals and recrystallization materials. While, the T_m1 for the PP corresponds to the melting of the dominant crystals formed during the first cooling process, indicating that addition of WF make the crystal more perfect.

XRD analysis

Figure 3 shows the XRD patterns of the samples which had the same thermal treatment as those presented in Fig. 1, respectively. When WF was added the diffraction intensity of PP at about $2\theta = 18.4°$ decreased with the increase of WF content, which indicated the planes of (040) and (130) in PP were preferential orientations.

It is well known that PP can crystallize into different crystal structures, which can exhibit different melting temperature. Therefore, the double melting behaviors of PP

were attributed to melting of different crystal forms or crystalline transitions during heating. No crystalline transition could be observed in the melting range of samples, as shown in Fig. 3.

The presence of the β-form of PP by reflection at $2\theta = 21.2°$ could be seen [42]. A comparison of the crystallographic reflections at scattering angles of 21.2° and 21.8° in Fig. 3, suggesting that WF could decrease the fraction of PP to crystallize in the β-form slightly. Clearly, the crystal structures were identical for all of the samples and the degree of crystallinity almost change with increasing WF content, as also evidenced by the similar DSC curves given in Fig. 1. For the neat PP, an almost amorphous halo with a few crystalline protrusions on the XRD pattern was only observed. With increasing WF content, the overall crystallinity or crystal perfection gradually increased, that is, the amount of amorphous fraction steadily decreased. The same phenomenon was observed in PP/nano-calcium carbonate by Huang et al. [42]. These results of XRD were in agreement with above DSC results presented in Fig. 1.

Melting behaviors following isothermal crystallization

The effect of WF and *m*-TMI-*g*-PP on the crystallization behavior of PP was examined by studying the isothermal crystallizing–melting of PP and its composites by DSC in the range 387–401 K. The heating DSC curves of samples after isothermal crystallization at indicated temperature are shown in Fig. 4. The DSC analysis of isothermally crystallized samples showed a single melting peak for PP and its composites. Thus, the cause of the single peak in the scans was due to the melting of the material crystallized at each temperature, and no recrystallization happens. The values of T_m, ΔH_m, and X_c calculated for PP and composites in the temperature range 387–401 K are summarized in Table 3. It is clear from Table 3, with increasing T_c, the T_m shifted to higher temperature. This behavior could be explained by the formation of more perfect crystals during crystallization. As a result of *m*-TMI-*g*-PP improving interaction adhesion between WF and PP, T_m was decreased. Compared with the crystallization isotherms at the same T_c (393 K), it was pointed out that the crystallization rate of PP in W40P60 was fastest, the values of T_m and ΔH_m was highest, supporting the occurrence of nucleating effect of WF, and this effect was decreased in W40P60M6, mainly as a consequence of the stronger WF–PP interactions due to the *m*-TMI-*g*-PP, as reported by our previous research [22], that restricted the mobility of PP chains and hindered the crystallization process, this suggested that *m*-TMI-*g*-PP modified the nucleation ability of WF. Meanwhile, the single peak T_m was more significant in composites, indicating less secondary crystallization growth took place during isothermal crystallization.

Conclusions

The effects of crystallization condition on the crystallization and multiple melting behaviors have been comparatively investigated for PP and its WF composites. The results obtained indicated that the presence of WF enhanced both the melt and crystallization of the PP by acting as a heterogeneous nucleation agent. The more the contents of WF, the more influence on the crystallization of PP. The PP showed either single or double melting endotherms, depending on their previous crystallization condition. PP showed double peaks and PP/WF exhibited single melting peak after non-isothermal crystallization at different cooling rate. The temperature of the lower melting peak (T_m1) results from the melting of lamellae with different perfectness under different conditions, and the higher melting temperature (T_m2) originate from the melting of the recrystallized crystals. Interestingly, an additional endothermic peak was observed for the composites at higher cooling rate at presence of *m*-TMI-*g*-PP. Both neat PP and its composites exhibited single melting behaviors after isothermal crystallization at the indicated crystallization temperature. The occurrence of the low temperature melting endotherm should correspond to the melting of the crystallites originally formed during a cooling scan. At the presence of *m*-TMI-*g*-PP, T_m and ΔH_m decreased. All the above showed *m*-TMI-*g*-PP improved the interaction between WF and PP.

Acknowledgements This study was financially supported by the National Natural Science Foundation of China (30972313) and the Fundamental Research Funds for the Central Universities (DL11CB03) and the young top-notch talent support program of Northeast Forestry University (YTTP-1011-11).

References

1. Bledzki AK, Gassan J. Composites reinforced with cellulose based fibres. Prog Polym Sci. 1999;24:221–74.
2. Ng ZS, Simon LC, Elkamel A. Renewable agricultural fibres as reinforcing fillers in plastics. J Therm Anal Calorim. 2009;96:85–90.
3. Pracella M, Chionna D, Anguillesi I, Kulinski Z, Piorkowska E. Functionalization, compatibilization and properties of polypropylene composites with hemp fibres. Compos Sci Technol. 2006;66:2218–30.
4. Karnani R, Krishnan M, Narayan R. Biofibre-reinforced polypropylene composites. Polym Eng Sci. 1997;37:476–83.
5. Bledzki AK, Letman M, Viksne A, Rence L. A comparison of compounding processes and wood type for wood fibre–PP composites. Compos Part A Appl Sci Manuf. 2005;36:789–97.

6. Sombatsompop N, Yotinwattanakumtorn C, Thongpin C. Influence of type and concentration of maleic anhydride grafted polypropylene and impact modifiers on mechanical properties of PP/wood sawdust composites. J Appl Polym Sci. 2005;97:475–84.
7. Renner K, Móczó J, Pukánszky B. Deformation and failure of PP composites reinforced with lignocellulosic fibers: effect of inherent strength of the particles. Compos Sci Technol. 2009;69:1653–9.
8. Hristov V, Vasileva S. Dynamic mechanical and thermal properties of modified poly(propylene) wood fiber composites. Macromol Mater Eng. 2003;288:798–806.
9. Dányádi L, Janecska T, Szabó Z, et al. Wood flour filled PP composites: compatibilization and adhesion. Compos Sci Technol. 2007;67:2838–46.
10. Felix JM, Gatenholm P. The nature of adhesion in composites of modified cellulose fibers and polypropylene. J Appl Polym Sci. 1991;42:609–20.
11. Kazayawoko M, Balatinecz JJ, Matuana LM. Surface modification and adhesion mechanisms in wood fibre–polypropylene composites. J Mater Sci. 1999;34:6189–99.
12. Zafeiropoulos NE, Williams DR, Baillie CA. Engineering and characterisation of the interface in flax fibre/polypropylene composite materials. Part I. Development and investigation of surface treatments. Compos Part A Appl Sci Manuf. 2002;33:1083–93.
13. Dányádi L, Móczó J, Pukánszky B. Effect of various surface modifications of wood flour on the properties of PP/wood composites. Compos Part A Appl Sci Manuf. 2010;41:199–206.
14. Lu JZ, Wu Q, Mcnabb HS. Chemical coupling in wood fibre and polymer composites: a review of coupling agents and treatments. Wood Sci Technol. 2000;32:88–104.
15. Gramlich WM, Gardner DJ, Neivandt JD. Surface treatments of wood–plastic composites (WPCs) to improve adhesion. J Adhes Sci Technol. 2006;20:1873–87.
16. Kim H-S, Lee B-H, Choi S-W, Kim S, Kim H-J. The effect of types of maleic anhydride-grafted polypropylene(MAPP) on the interfacial adhesion properties of bio-flour-filled polypropylene composites. Compos Part A Appl Sci Manuf. 2007;38:1473–82.
17. Bullions TA, Gillespie RA, Price-O'Brien J, et al. The effect of maleic anhydride modified polypropylene on the mechanical properties of feather fiber, kraft pulp, polypropylene composites. J Appl Polym Sci. 2004;92(6):3771–83.
18. Qiu WL, Takashi E, Takahiro H. Interfacial interaction, morphology, and tensile properties of a composite of highly crystalline cellulose and maleated polypropylene. J Appl Polym Sci. 2006;102:3830–41.
19. Carlborn K, Matuana LM. Functionalization of wood particles through a reactive extrusion process. J Appl Polym Sci. 2006;101:3131–42.
20. Qiu WL, Zhang FR, Endo T, et al. Isocyanate as a compatibilizing agent on the properties of highly crystalline cellulose/polypropylene composites. J Mater Sci. 2005;40:3607–14.
21. Karmarkar A, Chauhan SS, Jayant M, et al. Mechanical properties of wood–fiber reinforced polypropylene composites: effect of a novel compatibilizer with isocyanate functional group. Compos Part A Appl Sci Manuf. 2007;38:227–33.
22. Guo CG, Wang QW. Influence of *m*-isopropenyl-α, α-dimethylbenzyl isocyanate grafted polypropylene on the interfacial interaction of wood-flour/polypropylene composites. J Appl Polym Sci. 2008;5:3080–6.
23. Ryszard K, Maria WP. Flammability and fire resistance of composites reinforced by natural fibers. Polym Adv Technol. 2008;19:446–53.
24. Bouza R, Marco C, Ellis G, Martín Z, Gómez MA, Barral L. Analysis of the isothermal crystallization of polypropylene/wood flour composites. J Therm Anal Calorim. 2008;94(1):119–27.
25. Borysiak S. A study of transcrystallinity in polypropylene in the presence of wood irradiated with gamma rays. J Therm Anal Calorim. 2010;101:439–45.
26. Mantia FPL, Morreale M. Accelerated weathering of polypropylene/wood flour composites. Polym Degrad Stabil. 2008;93:1252–8.
27. Ma LC, Li LP, Guo CG. Influence of m-isopropenyl-α, α-dimethylbenzyl isocyanate and styrene on non-isothermal crystallization behavior of polypropylene. J Therm Anal Calorim. 2010;101(3):1101–9.
28. Maity J, Jacob C, Das CK, et al. Direct fluorination of Twaron fiber and the mechanical, thermal and crystallization behaviour of short Twaron fiber reinforced polypropylene composites. Compos Part A Appl Sci Manuf. 2008;39:825–33.
29. Svoboda P, Svobodova D, Slobodian P, et al. Crystallization kinetics of polypropylene/ethylene–octene copolymer blends. Polym Test. 2009;28:215–22.
30. Razavi-Nouri M, Ghorbanzadeh-Ahangari M, Fereidoon A, et al. Effect of carbon nanotubes content on crystallization kinetics and morphology of polypropylene. Polym Test. 2009;28:46–52.
31. Karger-Kocsis J. Polypropylene structure, blends and composites. London: Chapman and Hall; 1995.
32. Arbelaiz A, Fernandez B, Ramos JA, et al. Thermal and crystallization studies of short flax fibre reinforced polypropylene matrix composites: effect of treatments. Thermochim Acta. 2006;440:111–21.
33. Zafeiropoulos NE, Baillie CA, Matthews FL. A study of transcrystallinity and its effect on the interface in flax fibre reinforced composite materials. Compos Part A Appl Sci Manuf. 2001;32:525–43.
34. Girone's J, Pimenta MTB, Vilaseca F, et al. Blocked diisocyanates as reactive coupling agents: application to pine fiber–polypropylene composites. Carbohydr Polym. 2008;74:106–13.
35. Pracella M, Chionna D, Anguillesi I, Kulinski Z, Piorkowska E. Functionalization, compatibilization and properties of polypropylene composites with hemp fibres. Compos Sci Technol. 2006;66:2218–30.
36. Acha BA, Reboredo MM, Marcovich NE. Effect of coupling agents on the thermal and mechanical properties of polypropylene–jute fabric composites. Polym Int. 2006;55(9):1104–13.
37. Devaux E, Gérard JF, Bourgin P, Chabert B. Two-dimensional simulation of crystalline growth fronts in a polypropylene/glass–fibre composite depending on processing conditions. Compos Sci Technol. 1993;48:199–203.
38. Brandrup J, Immergut EH. Polymer handbook. 2nd ed. New York: Wiley-Interscience; 1975. p. 241–65.
39. Monasse B, Haudin JM. Growth transition and morphology change in polypropylene. Colloid Polym Sci. 1985;263:822–31.
40. Ke Y, Long CF, Qi ZN. Crystallization, properties, and crystal and nanoscale morphology of PET–clay nanocomposites. J Appl Polym Sci. 1999;71:1139–46.
41. Supaphol P, Thanomkiat P, Junkasem J, Dangtungee R. Non-isothermal melt-crystallization and mechanical properties of titanium(IV) oxide nanoparticle-filled isotactic polypropylene. Polym Test. 2007;26:20–37.
42. Huang YP, Chen GM, Yao Z, Li HW, Wu Y. Non-isothermal crystallization behavior of polypropylene with nucleating agents and nano-calcium carbonate. Eur Polym J. 2005;41:2753–60.